Published OnlineFirst September 26, 2012; DOI: 10.1158/0008-5472.CAN-12-1329



# FGFR3 Stimulates Stearoyl CoA Desaturase 1 Activity to Promote Bladder Tumor Growth

Xiangnan Du[1], Qian-Rena Wang[1], Emily Chan[2], Mark Merchant[2], Jinfeng Liu[3], Dorothy French[4], Avi Ashkenazi[1], and Jing Qing[1]

## Abstract

Fibroblast growth factor receptor 3 (FGFR3) belongs to a family of receptor tyrosine kinases that control cell proliferation, differentiation, and survival. Aberrant activation of FGFR3 via overexpression or mutation is a frequent feature of bladder cancer; however, its molecular and cellular consequences and functional relevance to carcinogenesis are not well understood. Through transcriptional profiling of bladder carcinoma cells subjected to short hairpin RNA knockdown of FGFR3, we identified a gene-signature linking FGFR3 signaling with *de novo* sterol and lipid biosynthesis and metabolism. We found that FGFR3 signaling promotes the cleavage and activation of the master transcriptional regulator of lipogenesis, sterol regulatory element-binding protein 1 (SREBP1/SREBF1), in a PI3K-mTORC1-dependent fashion. In turn, SREBP1 regulates the expression of key lipogenic enzymes, including stearoyl CoA desaturase 1 (SCD1/SCD). SCD1 is the rate-limiting enzyme in the biosynthesis of monounsaturated fatty acids and is crucial for lipid homeostasis. In human bladder cancer cell lines expressing constitutively active FGFR3, knockdown of SCD1 by siRNA markedly attenuated cell-cycle progression, reduced proliferation, and induced apoptosis. Furthermore, inducible knockdown of SCD1 in a bladder cancer xenograft model substantially inhibited tumor progression. Pharmacologic inhibition of SCD1 blocked fatty acid desaturation and also exerted antitumor activity *in vitro* and *in vivo*. Together, these findings reveal a previously unrecognized role of FGFR3 in regulating lipid metabolism to maintain tumor growth and survival, and also identify SCD1 as a potential therapeutic target for FGFR3-driven bladder cancer. *Cancer Res; 72(22); 5843–55. ©2012 AACR.*

## Introduction

FGFR3 belongs to a family of 4 structurally and functionally related receptor tyrosine kinases (RTK), which transduce signals from many of the 22 identified fibroblast growth factor (FGF) polypeptides in human (1–3). Upon ligand binding, FGF receptor 3 (FGFR3) undergoes dimerization and becomes autophosphorylated at specific tyrosine residues. This triggers receptor recruitment of adaptor proteins, such as FGFR substrate 2α (FRS2α), leading to activation of several downstream signaling cascades, including the canonical Ras-Raf-MAPK and PI3K-Akt-mTOR pathways (1–3). FGFR3 signaling plays critical roles during embryonic development and in the maintenance of tissue homeostasis, and regulates cell proliferation, differentiation, migration, and survival in a context-dependent manner (3, 4).

**Authors' Affiliations:** [1]Molecular Oncology, [2]Cancer Signaling and Translational Oncology, [3]Bioinformatics, and [4]Pathology, Genentech, Inc., South San Francisco, California

**Note:** Supplementary data for this article are available at Cancer Research Online (http://cancerres.aacrjournals.org/).

**Corresponding Author:** Jing Qing, Department of Molecular Oncology, Genentech, Inc., 1 DNA Way, South San Francisco, CA 94080. Phone: 650-467-8266; Fax: 650-467-8195; E-mail: jqing@gene.com

**doi:** 10.1158/0008-5472.CAN-12-1329



FGFR3 is implicated in diverse physiologic and pathologic conditions. Gain-of-function mutation in FGFR3 is one of the most common genetic alterations in a spectrum of human congenital skeletal and cranial disorders (5, 6). Activation of FGFR3 via mutations or overexpression is linked to a variety of human cancers, including multiple myeloma positive for t(4;14) (p16.3;q32) chromosomal translocation (7–10), bladder cancer (11–14), breast cancer (15), cervical carcinoma (11, 16), hepatocellular carcinoma (17), squamous non-small cell lung cancer (18, 19), and testicular tumors (20). In particular, somatic activating mutations in FGFR3 have been identified in 60% to 70% of papillary and 16% to 20% of muscle-invasive bladder tumors (13, 14, 21). Moreover, FGFR3 overexpression is frequently observed in superficial as well as advanced bladder cancers (12, 13, 22). Several studies show that pharmacologic or genetic intervention with FGFR3 inhibits bladder cancer cell proliferation in culture and tumor growth in animal models (12, 23–26). These studies suggest that a subset of bladder cancers harbor an oncogenic "addiction" to FGFR3, underscoring the importance of this receptor as a therapeutic target. Indeed, both monoclonal antibody- and small molecule-based FGFR3 inhibitors are currently in clinical investigation for cancer therapy (27, 28). However, despite these advances in developing FGFR3 inhibitors, little is known about how FGFR3 signaling contributes to carcinogenesis.

To gain insight into the mechanisms underlying the oncogenic role of FGFR3 in bladder cancer, we studied the changes in

Published OnlineFirst September 26, 2012; DOI: 10.1158/0008-5472.CAN-12-1329



gene-expression profiles that occur upon loss of FGFR3. Further interrogation of the specific changes showed that oncogenic FGFR3 signaling promotes *de novo* lipogenesis and fatty acid desaturation, via PI3K/mTORC1-dependent regulation of SREBP1. Furthermore, we found that SCD1-catalyzed fatty acid desaturation is crucial for FGFR3-dependent proliferation and survival of bladder cancer cells, thus identifying SCD1 as a potential therapeutic target for FGFR3-driven bladder cancer, and possibly other cancer types with FGFR3 activation.

## Materials and Methods

### Cell culture, siRNA transfection, and reagents

The human bladder cancer cell lines SW780, BFTC-905, and Cal29 were obtained from American Type Culture Collection. RT112 cells were purchased from German Collection of Microorganisms and Cell Cultures (DSMZ). RT112 cells stably expressing doxycycline-inducible short hairpins (shRNA) targeting FGFR3 or enhanced green fluorescent protein (EGFP) were described in our previous study (25). Bladder cancer cell lines UMUC-14 and TCC-97-7 were obtained as described (25). The cells were maintained with Dulbecco's Modified Eagle's Medium supplemented with 10% FBS (Sigma), 100 U/mL penicillin, 0.1 mg/mL streptomycin, and L-glutamine under conditions of 5% $CO_2$ at 37°C.

Rapamycin and phosphoinositide 3-kinase (PI3K) inhibitor LY294002 were obtained from Cell Signaling Technology. A potent and selective MEK1/2 inhibitor PD0325901 (Pfizer) was purchased from Synthesis Med Chem. SCD1 small molecule inhibitor A37062 was purchased from BioFine International.

All RNA interference experiments were carried out with ON-TARGETplus siRNAs (50 nmol/L, Dharmacon). Cells were transfected with Lipofectamine RNAiMax (Invitrogen), and cell proliferation or apoptosis were assessed 48 hours or 72 hours after transfection.

### Gene expression array and analyses

RT112 cells expressing doxycline-inducible shRNAs targeting FGFR3 or EGFP were grown in 1% FBS medium with or without doxycycline (1 μg/mL) for 48 hours. Total RNA from subconfluent cell cultures was isolated using RNAeasy kit (Qiagen). RNA quality was verified by running samples on an Agilent Bioanalyzer 2100, and samples of sufficient quality were profiled on Affymetrix HGU133-Plus_2.0 chips. All gene expression data set described in this study has been deposited into Gene Expression Omnibus database under the accession number GSE41035. See Supplementary Materials for details about Gene Ontology (GO) biologic process analysis.

### Quantitative RT-PCR analyses of mRNA expression level

To detect transcripts of SREBP1, SREBP2, FASN, SCD1, SQLE, and HMGCoA synthase, quantitative reverse transcriptase PCR (qRT-PCR) was conducted with predesigned Taqman gene Expression assays (Applied Biosystems). All reactions were conducted at least in duplicates. The relative amount of all mRNAs was calculated using the comparative CT method after normalization to human RPL19.

### Analyses of total fatty acid synthesis and SCD1 activity assay

Lipogenic activity was determined by monitoring the incorporation of [1,2-$^{14}$C] acetate (Perkin Elmer) into fatty acids as reported (29). The [$^{14}$C] radioactivity was normalized to sample protein content.

SCD1 activity was determined by monitoring the desaturation of [1-$^{14}$C] 18:0 stearate (American Radiolabeled Chemicals) or the incorporation of [1,2-$^{14}$C] acetate into monounsaturated fatty acid (MUFA). SCD1 activity was expressed as the ratio of oleic on stearic methyl ester acids or palmitoleic on palmitic methyl ester acids. See Supplementary Materials and Methods for details.

### Generation of SW780 stable cells expressing Dox-inducible SCD1 shRNA

Three independent SCD1 shRNAs were cloned into pGpHUSH lentiviral vector Genentech developed. Detailed information of the vector would be provided upon request. The sequence for SCD1 shRNAs used in the studies is as follows: shRNA1: 5′-GATCCCCCTACAAGAGTGGCTGAGTTTTCAAGAGAAACTCAGCCACTCTTGTAGTTTTTTGGAAA; shRNA2: 5′-GATCCCCCTACGGCTCTTTCTGATCATTCAAGAGATGATCAGAAAGAGCCGTAGTTTTTTGGAAA; shRNA3: 5′- GATCCCCGCACATCAACTTCACCACATTCAAGAGATGTGGTGAAGTTGATGTGCTTTTTTGGAAA. All constructs were confirmed by sequencing. An shRNA targeting β-galactosidase was used as a control. Lentiviral transduction and stable cell selection were conducted as described (25).

### Cell proliferation and apoptosis studies

For siRNA experiments, at 72 hours after transfection, cells were processed for [Methyl-$^{3}$H] thymidine incorporation. For doxycycline-inducible shRNA experiments, cells were treated with or without 1 μg/mL doxycyline for 72 hours before further incubation with [$^{3}$H] thymidine for 16 hours. For SCD1 small molecule inhibitor experiment, cells were treated with indicated concentration of A37062 in dimethyl sulfoxide (DMSO) or DMSO alone for 48 hours. Cell viability was assessed with CellTiter-Glo (Promega). Activation of caspase 3 and caspase 7 was measured with the Caspase-Glo 3/7 assay kit (Promega). Values are presented as mean ± SD of quadruplets. Data are representative of at least 3 independent experiments.

For cell-cycle analysis, cell suspensions were fixed in 70% ethanol and stained with 0.5 mL of propidium iodide and RNase staining buffer (BD Pharmingen) for 15 minutes at room temperature. For flow cytometry analysis of apoptosis, MitoTracker Red and Alexa Fluor 488-conjugated Annexin V were used to stain cells following manufacturer's instructions (Invitrogen). Flow cytometric data analysis and visualization were conducted using FlowJo v8.4 software (Tree Star, Inc.).

### Protein analyses

See Supplementary Materials and Methods for details.

### Xenograft studies

All studies were approved by Genentech's Institutional Animal Care and Use Committee. Female CB17 severe

Published OnlineFirst September 26, 2012; DOI: 10.1158/0008-5472.CAN-12-1329



combined immunodeficiency (SCID) mice, 6 to 8 weeks of age, were purchased from Charles River Laboratory. Female athymic nude mice were obtained from Harlan Laboratory. Mice were maintained under specific pathogen-free conditions. SW780 shRNA stable cells ($7 \times 10^6$) were implanted subcutaneously into the flank of CB17.SCID mice in a volume of 0.2 mL in HBSS/Matrigel (1:1 v/v, BD Biosciences). UMUC-14 cells ($5 \times 10^6$) were implanted into athymic nude mice without Matrigel. For efficacy studies, mice with tumors of a mean volume of 150 to 200 $mm^3$ were randomly grouped into treatment cohorts of 8 or 10. For shRNA studies, mice were given sucrose $H_2O$ alone or supplemented with 1 mg/mL doxycycline. SCD1 inhibitor A37062 (75 mg/kg) or the vehicle control was administered twice daily by oral gavage for 20 days. Body weights and caliper measurement were taken twice weekly, and tumor volume was calculated using the formula: $V = 0.5\ a \times b^2$, where $a$ and $b$ are the length and width of the tumor, respectively. Tumor volume results are presented as mean tumor volume $\pm$ SEM and data were analyzed by Student $t$ test.

To analyze fatty acid desaturation in tumor tissues and mouse plasma and liver, samples were collected at the end of the efficacy study (2 hours after the last dose) and snap frozen. Fatty acid profiling was conducted by Microbial ID, Inc using a standard sample preparation method for saponification and methylation. The fatty acid methyl esters were extracted and loaded onto the gas chromatograph for analysis. Desaturation index was expressed as the ratio of oleic on stearic methyl ester acids or palmitoleic on palmitic methyl ester acids.

### Immunohistochemistry analysis

See Supplementary Materials and Methods for details.

### Statistics

Pooled data are expressed as mean $\pm$ SEM. Unpaired Student $t$ tests (2-tailed) were used for comparison between 2 groups. A value of $P < 0.05$ was considered statistically significant in all experiments other than microarray data analysis.

## Results

### FGFR3 knockdown inhibits fatty acid synthesis and desaturation

Using doxycycline-inducible shRNA, we previously showed that knockdown of FGFR3 in bladder cancer RT112 cells significantly attenuated tumor growth *in vitro* and *in vivo* (25). To identify potential oncogenic mediators that operate downstream of FGFR3, we determined the transcriptional profile of RT112-derived cell lines that express endogenous or depleted levels of FGFR3. To control for nonspecific differences, we compared independently established stable cell lines transduced with doxycycline-inducible control shRNA versus 3 independent FGFR3 shRNAs. All cell lines were treated with or without doxycycline for 48 hours to deplete FGFR3 protein before the isolation of mRNA for microarray analysis (Fig. 1A). Genes that were differentially expressed after doxycycline induction (false discovery rate <0.1, fold change >1.5) in all 3 FGFR3-depleted cell lines but not in the control cell line were considered potential FGFR3-regulated genes (Supplementary Fig. S1A). Among the 19,701 genes represented on the microarray, 313 showed consistent differential expression in response to FGFR3 knockdown, of which 196 were upregulated and 117 were downregulated (Fig. 1A, Supplementary Fig. S1A, and Supplementary Table S1).

Functional classification of the upregulated genes upon FGFR3 knockdown (Supplementary Table S1) did not reveal significant perturbation of any biologic process. In contrast, a large fraction of the downregulated genes by FGFR3 shRNAs encode a cohort of enzymes and proteins involved in fatty acid and sterol biosynthesis and metabolism (Fig. 1B and Supplementary Fig. S1B). SCD1, a rate-limiting enzyme that catalyzes the conversion of saturated fatty acids into MUFAs (30), was among the genes showing the biggest decline (down by 3.85-fold, Fig. 1B). This gene cluster also included fatty acid synthase (FASN; Fig. 1B). The microarray results were further confirmed using qRT-PCR analysis of the mRNA abundance of several representative genes (Supplementary Fig. S2). In addition, the FGFR3-dependent regulation of these lipogenic genes was also verified in bladder cancer cell line UMUC-14 treated either with a specific anti-FGFR3 monoclonal antibody (Supplementary Fig. S3A), or with short-interfering RNA-mediated FGFR3 knockdown (Supplementary Fig. S3B and S3C). Together, these data suggest that FGFR3 signaling exerts major transcriptional control over a cohort of genes involved in sterol and lipid biosynthesis and metabolism.

Because it is well established that many genes involved in sterol and lipid biosynthesis are regulated by the SREBP family of master transcription factors (31, 32), and SREBP1 itself displayed modest downregulation in the current microarray study (down by 1.46-fold, data not shown), we examined the levels of SREBP1 and SREBP2 mRNA using qRT-PCR. FGFR3 knockdown in RT112 cells decreased SREBP1 mRNA levels by about 50%, and did not affect SREBP2 mRNA level (Supplementary Fig. S2C). Similar results were observed in UMUC-14 cells transfected with FGFR3 siRNA (Supplementary Fig. S3D). These data raise the possibility that FGFR3 may regulate *de novo* lipogenesis through SREBP1.

SREBP1 activity is tightly regulated by intracellular sterol level. In response to cholesterol deprivation, SREBP1 undergoes proteolytic N-terminal processing and consequent nuclear translocation of the cleaved mature fragment, leading to the transcriptional induction of lipogenic enzymes (33). FGFR3 knockdown diminished the full-length as well as the cleaved, mature form of SREBP1, but had a minimal detectable effect on either form of SREBP2 (Fig. 1C). A modest reduction in FASN and a pronounced decrease in SCD1 levels were apparent in cells expressing FGFR3 shRNA, but not control shRNA (Fig. 1C). Further analysis of RT112 cells metabolically labeled with [1,2-$^{14}$C]acetate revealed a marked decrease in fatty acid synthesis upon FGFR3 knockdown (Fig. 1D).

Given that FGFR3 knockdown nearly abolished the expression of SCD1, the rate-limiting enzyme in the biosynthesis of MUFAs, we examined the effect of FGFR3 depletion on fatty acid desaturation using [$^{14}$C]stearic acid labeling. FGFR3 shRNA blocked the production of unsaturated oleic acid from

Published OnlineFirst September 26, 2012; DOI: 10.1158/0008-5472.CAN-12-1329



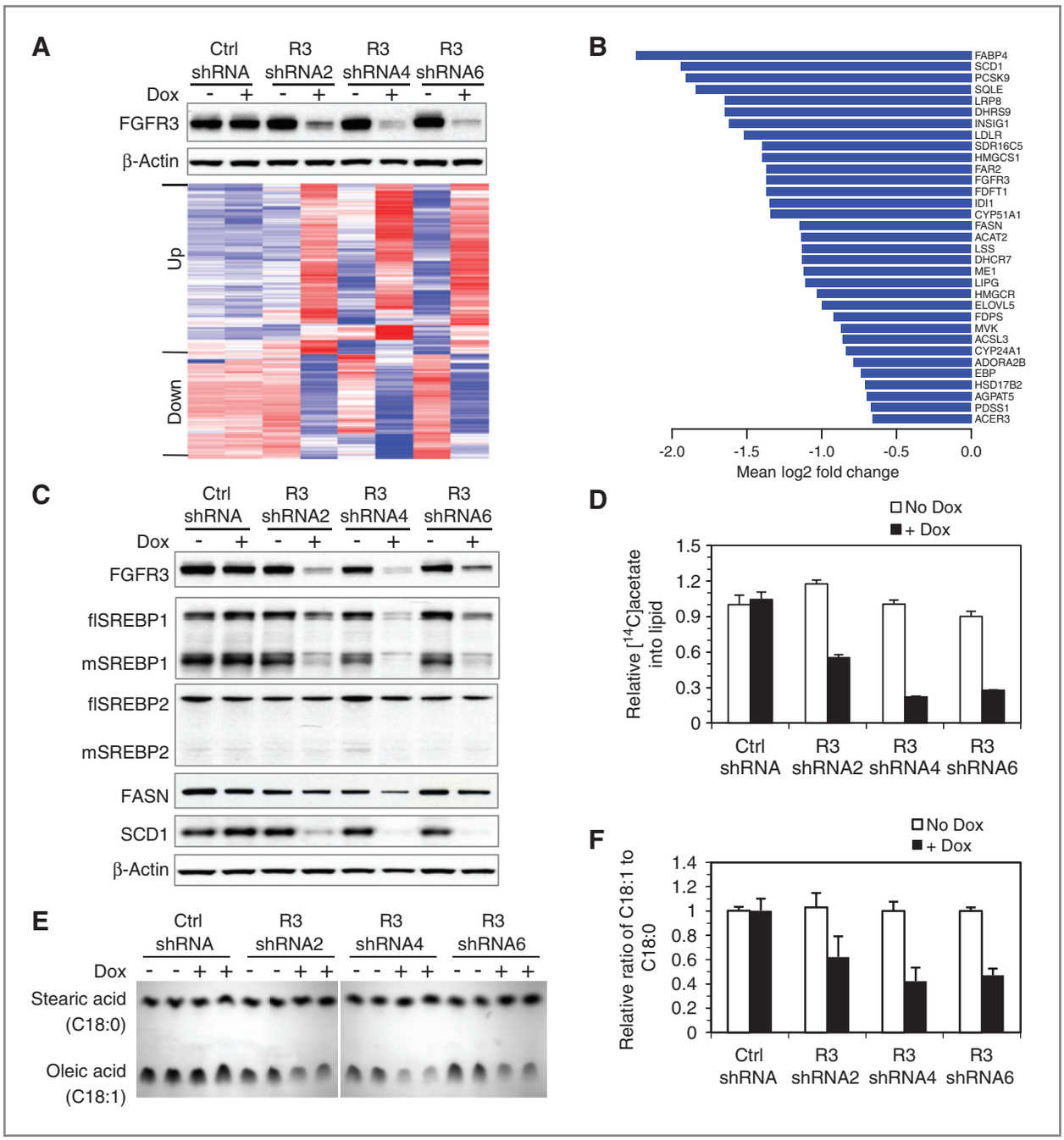


**Figure 1.** FGFR3 knockdown reduces fatty acid synthesis and desaturation. A, heat map of the probes found to be regulated by FGFR3 knockdown. RT112 bladder cancer cells expressing 3 independent doxycycline-inducible FGFR3 shRNAs or a control shRNA (Ctrl) were cultured with or without 1 μg/mL doxycycline for 2 days before RNA extraction. Total RNA was subjected to microarray studies. Genes that are regulated by all 3 FGFR3 shRNAs are shown in the heat map. Top panel shows FGFR3 protein level. B, a cohort of genes involved in cholesterol and lipid biosynthesis is repressed by FGFR3 knockdown. C, FGFR3 knockdown reduces the expression of SREBP1, FASN, and SCD1. RT112 cells were cultured with or without 1 μg/mL doxycycline for 3 days before harvest. Cell lysates were subjected to immunoblot analyses. flSREBP, full-length SREBP; mSREBP, mature processed SREBP. D, FGFR3 knockdown suppresses lipid biosynthesis. RT112 cells were cultured with or without 1 μg/mL doxycycline for 3 days before 4 hours incubation with [$^{14}$C]acetate. The lipid fraction was extracted and [$^{14}$C]acetate incorporated into lipids was measured by scintillation counting. Data were normalized to sample protein content, and presented as mean ±SD ($n = 3$). E, FGFR3 knockdown blocks stearic acid desaturation. RT112 cells were treated as in D before 6 hours incubation with [$^{14}$C]stearic acid. [$^{14}$C]stearic acid desaturation was analyzed by argentation thin layer chromatography. F, relative ratio of oleic acid (C18:1) to stearic acid (C18:0) measured by scintillation counting of fatty acid in E. Data are presented as ±SD of mean from 3 independent experiments.

Published OnlineFirst September 26, 2012; DOI: 10.1158/0008-5472.CAN-12-1329



the saturated stearic acid precursor, whereas the control shRNA had no effect (Fig. 1E and F). Together, these results suggest that FGFR3 signaling is important for controlling *de novo* synthesis and desaturation of fatty acids, by maintaining expression and activity of SREBP1 and hence the induction of key lipogenic enzymes including FASN and SCD1.

### FGFR3 signaling activates SREBP1 and promotes SCD1-mediated fatty acid desaturation mainly through PI3K-mTORC1

To dissect out the molecular circuitry underlying FGFR3 regulation of *de novo* fatty acid synthesis and desaturation, we activated FGFR3 signaling in bladder cancer cells with FGF1 and analyzed SREBP1 expression and cleavage. Cal29 bladder cancer cells express high levels of endogenous FGFR3, and FGF1 treatment of these cells induced robust phosphorylation and activation of FGFR3 and downstream signaling effectors in a time- and dose-dependent manner (Fig. 2A and Supplementary Fig. S4A). Although FGF1 did not affect full-length inactive SREBP1 protein levels, the cleaved, mature form of SREBP1 was substantially more abundant after 2 hours of FGF1 treatment and sustained at 24 hours and 48 hours (Fig. 2A and data not shown); in contrast, the effect on full-length SREBP2 protein level and its processing is minimal. Similarly, the level of SCD1, and to a lesser extent, FASN, was upregulated by FGF1 (Fig. 2A). Consistent with these changes, both saturated and unsaturated fatty acids were induced by FGF1 after a 24-hour incubation (Fig. 2B). Similar results, albeit with slower kinetics, were obtained in RT112 cells, where FGF1 induced a modest elevation in full-length SREBP1, an accumulation of mature SREBP1 peaking approximately 24 hours posttreatment, and an increased synthesis of both saturated and unsaturated fatty acids (Supplementary Fig. S4B–S4D).

To determine whether the induction of SCD1 by FGF1 depends on SREBP1, we depleted SREBP1 or SREBP2 using specific siRNAs in RT112 cells. SREBP1 knockdown markedly

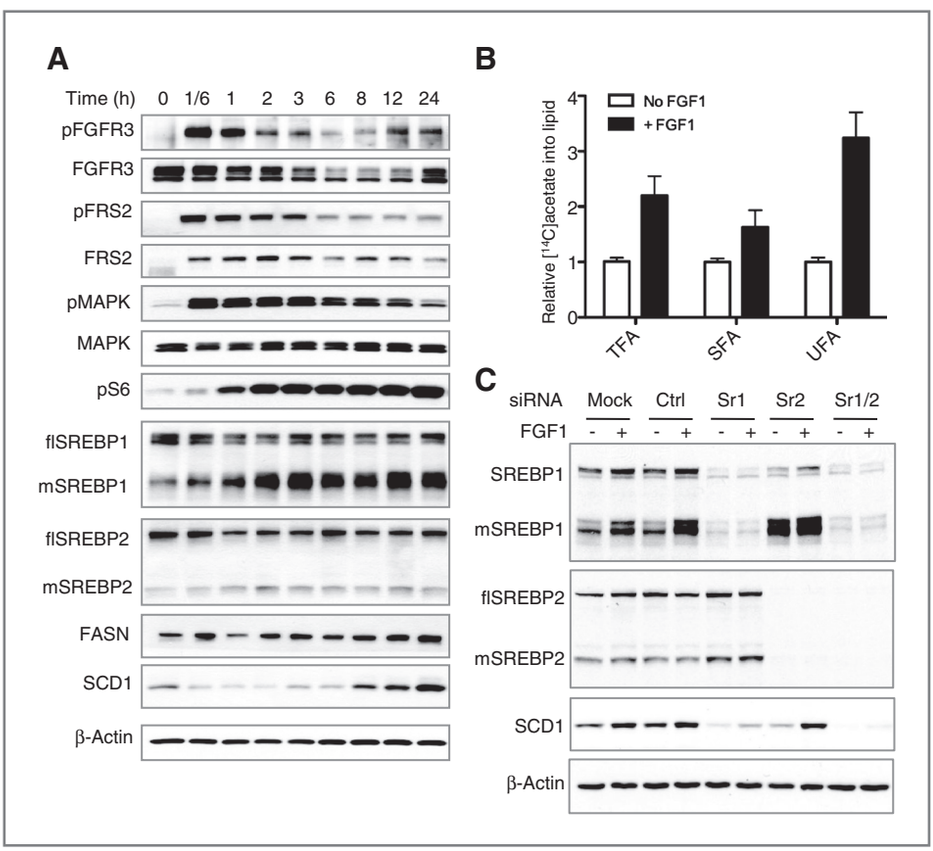


Figure 2. FGFR3 signaling promotes fatty acid synthesis and desaturation in an SREBP1-dependent manner. A, FGF1-FGFR3 axis stimulates the accumulation of matured SREBP1 and the expression of FASN and SCD1. Cal29 bladder cancer cells were serum starved for 20 hours, then treated with FGF1 (25 ng/mL) and heparin (10 μg/mL) for indicated time. Cell lysates were immunoprecipitated with anti-FGFR3 antibody and assessed for FGFR3 phosphorylation with an antiphospho-tyrosine antibody (4G10). Lysates were also immunoblotted to detect indicated proteins as described in Materials and Methods. flSREBP, full-length SREBP; mSREBP, mature processed SREBP. B, FGF1 stimulates fatty acid synthesis and desaturation in Cal29 cells. Cal29 cells were serum starved for 20 hours, then incubated with 25 ng/mL of FGF1 and 10 μg/mL of heparin for 24 hours. [$^{14}$C]acetate was added for another 16 hours incubation. $^{14}$C incorporation into total fatty acid (TFA), saturated fatty acids (SFA), and unsaturated fatty acids (UFA) was measured by scintillation counting. Data were normalized to sample protein content and presented as mean of triplicates ±SD relative to no FGF1 treatment and are representative of 2 independent experiments. C, FGF1 stimulates SCD1 expression mainly through SREBP1. RT112 cells were transfected with siRNA targeting SREBP1 (Sr1), SREBP2 (Sr2), or a nontargeting control siRNA (Ctrl). At 24 hours after transfection, cells were serum starved for 20 hours, then treated with FGF1 (25 ng/mL) and heparin (10 μg/mL) for 24 hours. Total cell lysates were subjected to immunoblot analyses.

Published OnlineFirst September 26, 2012; DOI: 10.1158/0008-5472.CAN-12-1329



reduced both basal and FGF1-induced SCD1 mRNA (data not shown) and protein expression, whereas SREBP2 siRNA alone had minimal effect (Fig. 2C). Of note, knockdown either SREBP protein led to a modest increase in the expression of the mature form of the other protein, suggesting a potential compensatory regulation loop. Importantly, targeting both SREBP1 and SREBP2 together almost completely abolished SCD1 expression at both mRNA (data not shown) and protein level (Fig. 2C), suggesting that although SREBP1 plays a dominant role, both transcription factors contribute to maximal SCD1 induction in response to FGF1 stimulation.

To assess the involvement of specific signaling mediators downstream of FGFR3 in the regulation of fatty acid synthesis and desaturation, we blocked canonical FGFR3 signaling at various nodes using the PI3K inhibitor Ly294002, the mTORC1 inhibitor rapamycin, and the MEK1/2 inhibitor PD325901. In RT112 bladder cancer cells, each inhibitor blunted FGF1-induced activation of the intended target(s), as assessed by the phosphorylation of AKT, S6 kinase, or mitogen-activated protein kinase (MAPK), respectively (Fig. 3A). Although the inhibitors elicited minimal effect on the expression of full-length SREBP1 protein, they all substantially reduced both the basal and the FGF1-induced levels of cleaved, active SREBP1 (Fig. 3B). Coordinately, SCD1 expression was diminished significantly by each of the inhibitors, with the PI3K inhibitor showing the strongest effect. FASN expression was reduced only modestly by each of the compounds (Fig. 3B). Treatment of RT112 cells with the inhibitors suppressed both basal and FGF1-stimulated synthesis of total, as well as unsaturated fatty acids (Fig. 3C and D). Consistent with these results, in Cal29 bladder cancer cells, Ly294002 and rapamycin also blocked the accumulation of active SREBP1 and the expression of SCD1, but the selective MEK1/2 inhibitor PD325901 only partially attenuated FGF1-indcued accumulation of active SREBP1, and

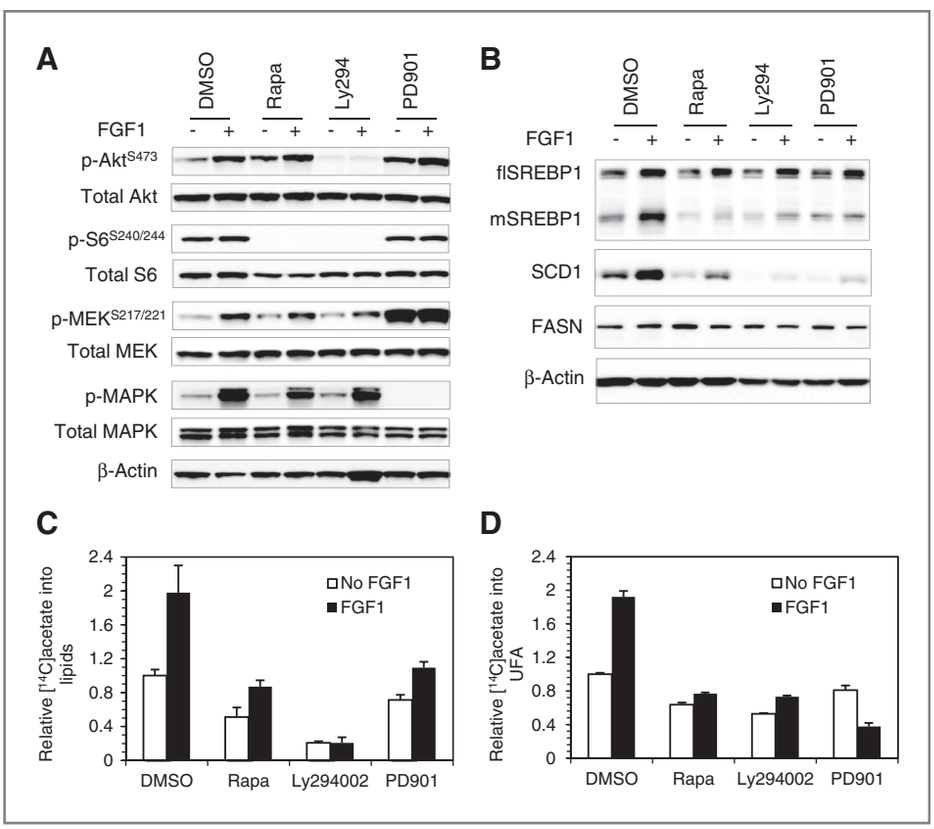


Figure 3. FGFR3 signaling promotes the accumulation of matured SREBP1 and fatty acid desaturation via PI3K-mTORC1 pathway. A, pharmacologic inhibition of FGFR3 signaling. RT112 cells were serum starved for 20 hours, then treated with rapamycin (50 nmol/L), Ly294002 (Ly294, 20 μmol/L), and PD325901(PD901,100 nmol/L) for 2 hours, followed by stimulation with 30 ng/mL FGF1 plus 10 μg/mL of heparin for 10 minutes. Cell lysates were subjected to immunoblot analyses with indicated antibodies. Note the increased phosphorylation of MEK upon PD901 treatment, presumably because of a relief of feedback inhibition. B, PI3K-mTORC1 and MEK inhibitors block FGF1 induction of SREBP1 and SCD1 in RT112 cells. RT112 cells were serum starved for 20 hours, treated with kinase inhibitors for 4 hours, followed by 24 hours incubation in medium supplemented with 30 ng/mL FGF1. Cell lysates were immunoblotted to detect full-length (fl) and mature (m) SREBP1, SCD1, and FASN protein levels. C, PI3K-mTORC1 and MEK inhibitors block FGF1-stimulated synthesis of total lipids. RT112 cells were treated the same as described in B. [$^{14}$C]acetate was added for the final 4 hours incubation. The lipid fraction was extracted and [$^{14}$C]acetate incorporated into total lipids was measured by scintillation counting. Data were normalized to sample protein content and presented as mean of triplicates ±SD. These data are representative of 2 independent experiments. D, PI3K-mTORC1 and MEK inhibitors block FGF1-stimulated synthesis of unsaturated fatty acids (UFA). RT112 cells were treated as in C, and unsaturated fatty acids were analyzed by argentation thin layer chromatography and quantitated by scintillation counting. Data are presented as mean of triplicates ±SD, and are representative of 3 independent experiments.

Published OnlineFirst September 26, 2012; DOI: 10.1158/0008-5472.CAN-12-1329



had little effect on SCD1 induction (Supplementary Fig. S5). Thus, FGFR3 signals mainly through the PI3K-mTORC1 axis in bladder cancer cells to promote SREBP1 processing and activation, stimulating *de novo* synthesis and desaturation of fatty acids. The MEK-MAPK pathway may also contribute to this function in a context-dependent manner.

### SCD1 knockdown blocks cell-cycle progression and induces apoptosis preferentially in bladder cancer cells with active FGFR3 signaling

It has been postulated that certain cancer types, including breast and prostate carcinoma as well as glioblastoma, require *de novo* fatty acid synthesis for uncontrolled cell proliferation and survival (34). To examine the importance of FGFR3-stimulated lipogenesis for bladder tumor growth and to explore the potential of the lipogenic pathway as a therapeutic target, we examined the impact of siRNA-mediated knockdown of SREBP1, FASN, or SCD1 on cell proliferation. Our initial studies revealed that SCD1 knockdown elicited the strongest antiproliferative effect (data not shown); we therefore chose to investigate SCD1 further using a panel of bladder cancer cells lines (Supplementary Table S2). UMUC-14 and TCC-97-7 cells harbor $FGFR3^{S249C}$, the most frequent activating mutation found in FGFR3 (25, 35). Although SW780 cells possess wild type FGFR3 (26; data not shown), they display constitutive phosphorylation and activity of FGFR3 and FRS2 (Supplementary Fig. S6A). SCD1 knockdown markedly suppressed DNA synthesis as measured by [$^3$H]thymidine incorporation in cell lines with constitutively activated FGFR3, namely UMUC-14, TCC-97-7, and SW780 (Fig. 4A). In contrast, in cell lines with wild type FGFR3, SCD1 knockdown inhibited proliferation of Cal29 cells by about 40% to 50%, but did not affect this endpoint in RT112 and BFTC-905 cells (Fig. 4B). The lack of response of RT112 and BFTC-905 cells to SCD1 knockdown is not due to a slower growth rate or senescence under the current experimental conditions (Supplementary Fig. S6B). These results suggested that bladder cancer cells with constitutively activated FGFR3 signaling rely more heavily on SCD1 activity for proliferation.

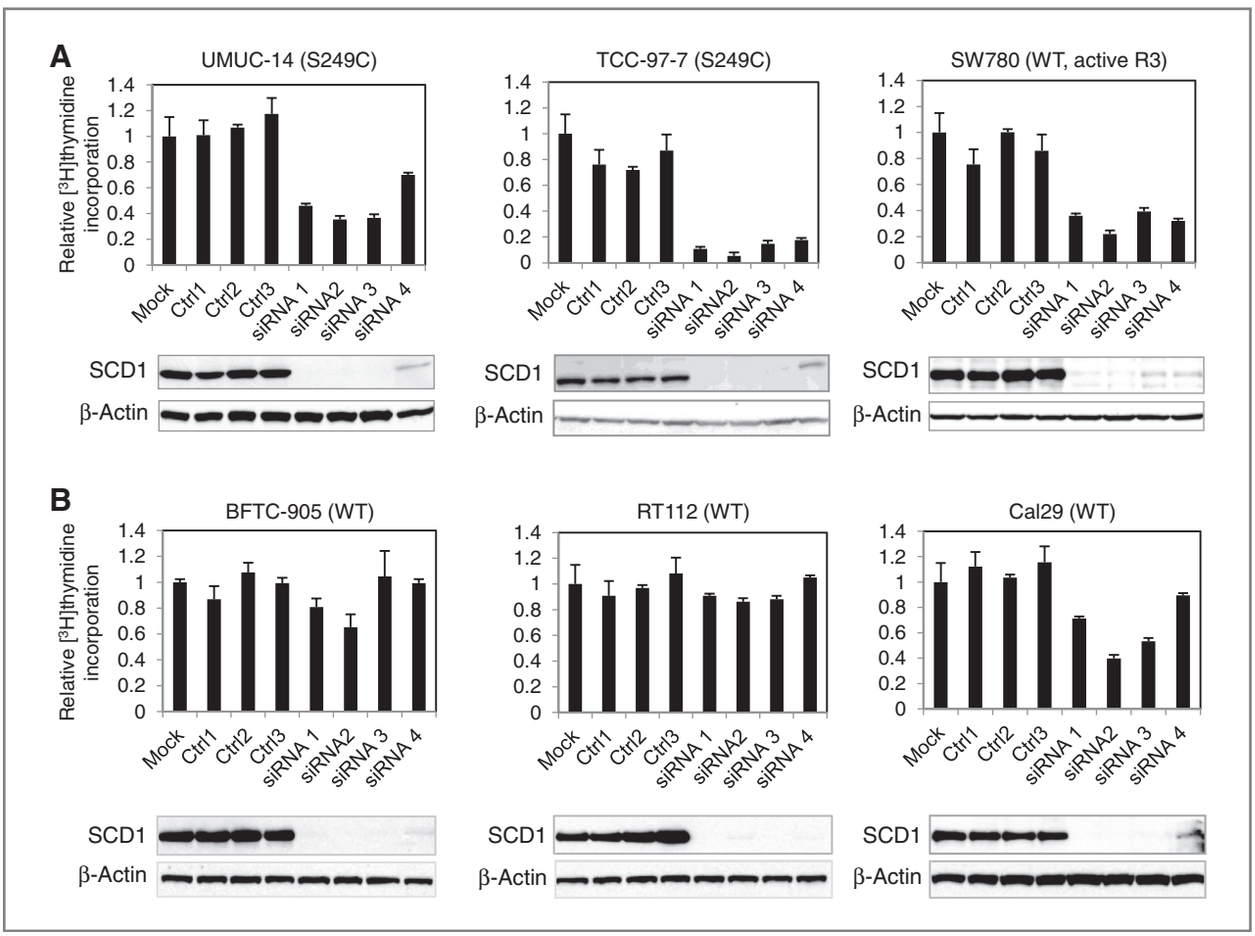


Figure 4. Constitutive FGFR3 signaling sensitizes bladder cancer cells to SCD1 knockdown. A panel of bladder cancer cells with constitutive FGFR3 signaling (A) or ligand-dependent activation of FGFR3 (B) were grown in medium containing 1% FBS, transfected with SCD1 siRNAs or 3 nontargeting control siRNAs (Ctrl), and cell proliferation was measured by [$^3$H]thymidine incorporation at 72 hours after transfection. Data are presented as mean of triplicates ±SD relative to cells transfected with RNAiMax alone (Mock) and are representative of 3 independent experiments. Bottom, representative Western blots showing SCD1 protein level in siRNA transfected cells.

Published OnlineFirst September 26, 2012; DOI: 10.1158/0008-5472.CAN-12-1329



Further analyses of exponentially growing SW780 cells revealed that at 48 hours post-SCD1 knockdown, the percentage of cells in the $G_2$ and S-phases of the cell cycle was substantially and specifically reduced, with concomitant increase in the percentage of cells in $G_1$ (Fig. 5A). Because a subdiploid population started to appear at 72 hours post-SCD1

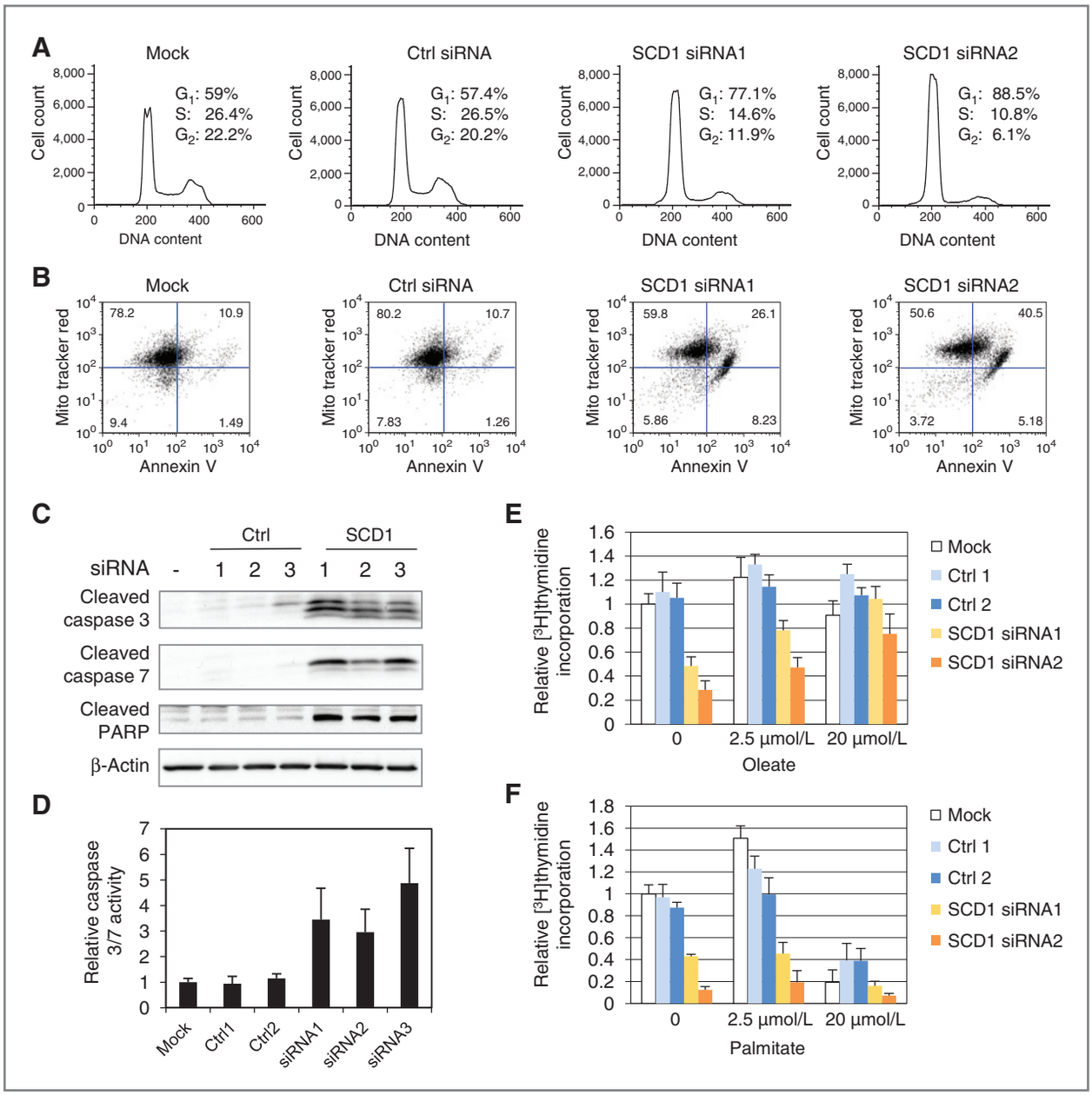


Figure 5. SCD1 knockdown inhibits cell proliferation and induces apoptosis in a fatty acid desaturation-dependent manner. A and B, SCD1 knockdown leads to $G_1$ cell-cycle arrest and apoptosis. SW780 cells were transfected with SCD1 siRNAs or a nontargeting control siRNA (Ctrl), and cell-cycle analysis (A) or Annexin V staining (B) was conducted at 48 hours after transfection as described in Materials and Methods. Data are representative of 3 independent experiments. C and D, SCD1 knockdown induces caspases 3/7 cleavage and activation. SW780 cells were transfected with SCD1 siRNAs or nontargeting control siRNAs (Ctrl), and cell lysates were subjected to immunoblot analysis (C). Activities of caspases 3 and 7 were measured with Caspase-Glo 3/7 assay kit (Promega; D). E, monounsaturated oleate rescues SW780 cells from SCD1 knockdown. Cells grown in medium containing 1% FBS were transfected with SCD1 siRNAs or nontargeting control siRNAs (Ctrl). At 6 hours after transfection, bovine serum albumin-conjugated oleate acid was added to the culture medium as indicated. Cell proliferation was measured by [$^3$H]thymidine incorporation at 72 hours posttreatment. Data are presented as mean of triplicates ±SD relative to cells transfected with RNAiMax alone (Mock) and grown in medium supplemented with bovine serum albumin only. Data are representative of 3 independent experiments. F, saturated palmitate is unable to reverse the effect of SCD1 siRNAs. Cells were treated similarly as described in E, except that bovine serum albumin-conjugated palmitate was supplemented at 6 hours post-siRNA transfection. Similar results were observed in UMUC-14 cells (Supplementary Fig. S7).

Published OnlineFirst September 26, 2012; DOI: 10.1158/0008-5472.CAN-12-1329



knockdown (data not shown), we analyzed the effect of SCD1 siRNAs on apoptosis. SCD1 knockdown in SW780 (Fig. 5B) and UMUC-14 cells (Supplementary Fig. S6C) significantly increased FACS staining for the apoptotic cell-surface marker Annexin-V. Furthermore, SCD1 knockdown led to cleavage of caspases-3 and -7, as well as the caspase-3 substrate PARP (Fig. 5C), and elevated caspases-3/7 enzymatic activity (Fig. 5D and Supplementary Fig. S6D and S6E). Hence, in bladder cancer cells harboring constitutively activated FGFR3, loss of SCD1 inhibits cell-cycle progression and stimulates apoptosis.

### SCD1 siRNAs inhibit cell proliferation in a fatty acid desaturation-dependent manner

Next, we assessed the effect of SCD1 siRNAs on fatty acid desaturation using argentation thin-layer chromatography. SCD1 knockdown markedly blocked the conversion of [$^{14}$C]stearate into [$^{14}$C]oleate, whereas the nonspecific control siRNAs or FASN siRNAs had no effect (Supplementary Fig. S7A and S7B). We reason that if the inhibition of cell proliferation upon SCD1 knockdown is due to deficient production of MUFAs, then exogenously provided oleate should rescue this inhibition. Indeed, oleate supplements reversed SCD1 siRNA-mediated growth inhibition in a dose-dependent manner, whereas palmitate add-back failed to rescue the growth-inhibitory effect in both SW780 and UMUC-14 cells (Fig. 5E and F; Supplementary Figure S7C and S7D). Of note, a high concentration of palmitate (20 μmol/L) was detrimental to the viability of these cells (Fig. 5F; Supplementary Fig. S7D). Hence, fatty acid desaturation by SCD1 is essential for growth of bladder cancer cells driven by constitutively active FGFR3.

### Doxycycline-inducible knockdown of SCD1 attenuated tumor growth *in vivo*

To evaluate the effect of SCD1 knockdown on tumor growth *in vivo*, we established stable SW780 cells expressing doxycycline-inducible SCD1 shRNA. Induction of 3 independent SCD1 shRNAs by doxycycline diminished SCD1 protein expression, with shRNA1 and shRNA3 showing strongest downregulation, whereas expression of a control shRNA targeting β-galactosidase had no effect on SCD1 (Fig. 6A). Doxycycline treatment

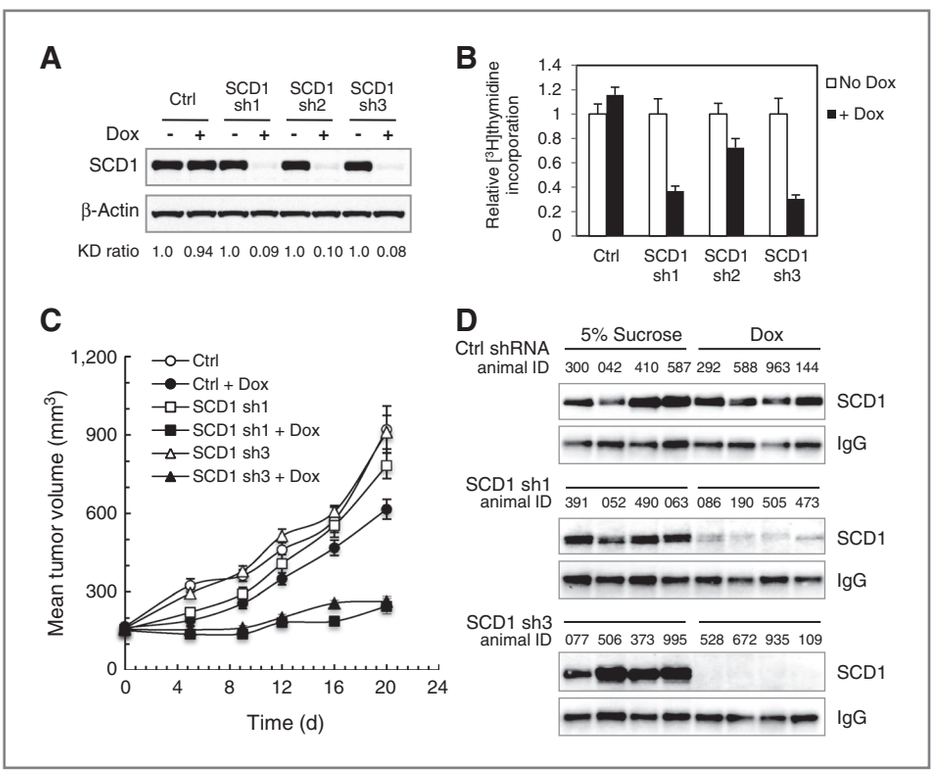


Figure 6. Doxycycline-inducible knockdown of SCD1 in SW780 bladder caner cells suppresses tumor growth *in vivo*. Three different SCD1 shRNAs were cloned into a Tet-inducible lentiviral expression vector. SW780 cells stably expressing doxycycline-inducible SCD1 shRNA or a control shRNA (Ctrl) were established with puromycin selection. A, representative blots showing SCD1 expression in stable cells treated with or without 1 μg/mL doxycycline (Dox) for 3 days. KD ratio indicates the efficiency of SCD1 knockdown relative to cells without Dox treatment. B, SCD1 knockdown reduces [$^3$H]thymidine incorporation. SW780 cells were cultured with or without 1 μg/mL Dox for 3 days before 16 hours incubation with [$^3$H]thymidine. Counts of incorporated [$^3$H]thymidine were presented as mean of triplicates ±SD relative to cells without Dox treatment. C, SCD1 knockdown attenuates tumor growth in mice. SW780 cells expressing SCD1 shRNA1 and 3 or a control shRNA (Ctrl) were inoculated into CB.17 SCID mice and grouped out into cohorts of 10 for treatment. Mice were given 5% sucrose alone or supplemented with 1 mg/mL Dox, and tumor size was measured twice a week. Tumor volume is presented as mean ± SEM. At day 20, for SCD1 shRNA1 (with vs. without Dox), $P < 0.0001$; for SCD1 shRNA3 (with vs. without Dox), $P < 0.0001$. At day 20, in the presence of Dox, shRNA 1 versus Ctrl shRNA, $P < 0.0001$; shRNA3 versus Ctrl shRNA, $P < 0.0001$. D, expression of SCD1 protein in tumor lysates extracted from control or SCD1 shRNA xenograft tissues. Tumor lysates were immunoprecipitated with anti-SCD1 antibody and evaluated for SCD1 protein level by immunoblot.

Published OnlineFirst September 26, 2012; DOI: 10.1158/0008-5472.CAN-12-1329



reduced [$^3$H]thymidine incorporation by cells expressing SCD1 shRNAs (Fig. 6B), confirming that SCD1 knockdown inhibits cell proliferation.

We next evaluated the effect of SCD1 shRNAs on the growth of preestablished SW780 tumor xenografts in SCID mice. Although in cell expressing control shRNA, doxycycline itself appeared to reduce tumor growth by about 30%, SCD1 knockdown substantially and significantly suppressed tumor growth as compared with cells expressing the control shRNA (Fig. 6C). Analysis of tumor samples on day 20 confirmed effective and sustained SCD1 knockdown upon doxycycline induction (Fig. 6D). These results show that SCD1 is critically important for the growth of SW780 bladder cancer cells both *in vitro* and *in vivo*.

### Pharmacologic inhibition of SCD1 attenuates UMUC-14 tumor growth and reduces fatty acid desaturation in mice

To examine further the importance of fatty acid desaturation for FGFR3-driven bladder tumor growth, we blocked the enzymatic activity of SCD1 pharmacologically, using the commercially available small molecule inhibitor A37062. This compound blocked the conversion of [$^{14}$C]stearate into [$^{14}$C]oleic acid (data not shown), and suppressed the synthesis of MUFA from [$^{14}$C]acetate, with an estimated $IC_{50}$ value of 30 nmol/L (Fig. 7A). Treatment of UMUC-14 cells, which harbor $FGFR3^{S249C}$ mutation endogenously, with the SCD1 inhibitor promoted the processing and activation of effector caspases-3 and -7, as well as cleavage of PARP (Fig. 7B). Under normal growth conditions, 100 nmol/L A37062 reduced the viability of UMUC-14 cells by approximately 85% (Fig. 7C and D). Exogenously supplemented oleate reversed this effect in a dose-dependent fashion, whereas palmitate had no effect (Fig. 7C and D). Similar results were obtained in SW780 cells (Supplementary Fig. S8). These data indicate that A37062 inhibits bladder cancer cell survival by inhibiting SCD1-mediated generation of MUFAs.

Next, we examined the effect of A37062 on the growth of preestablished bladder cancer xenografts *in vivo*. Athymic nude mice harboring UMUC-14 tumors were dosed twice a day with vehicle or A37062 (75 mg/kg) for 20 days. Compared with vehicle control at day 20, A37062 suppressed tumor growth by about 60% (Fig. 7E). Immunohistochemistry (IHC) analysis of Ki-67 status in tumor tissues harvested at day 20 suggested a trend of lower cell proliferation index in A37062-treated samples compared with vehicle-treated group, but this reduction was not statistically significant (data not shown). We also evaluated apoptosis induction in UMUC-14 tumors in a separate study looking at cleaved caspases 3 (by IHC). Treatment with A37062 for 4 days increased the staining of cleaved caspase 3 significantly (Supplementary Fig. S9). These data suggest that the predominant effect of SCD1 inhibition in the UMUC-14 xenograft model is mediated through apoptosis induction.

Analysis of tumor lysates collected at 2 hours after the last dose showed that A37062 markedly decreased the ratio of monounsaturated to saturated fatty acids in tumors (Fig. 7F and G). Similarly, analysis of liver tissue and plasma showed significantly attenuated fatty acid desaturation (Fig. 7F and G). Thus, A37062 inhibits growth of UMUC-14 tumor xenografts *in vivo* in conjunction with a blockade in fatty acid desaturation. Of note, we did not observe any significant weight loss or other gross abnormalities in the mice in the course of these experiments, suggesting that SCD1 inhibition was well tolerated in nude mice.

## Discussion

Bladder cancer is the 5th most common cancer worldwide, with an estimated 70,530 new cases and 14,680 deaths in 2010 in the United States (36). A high prevalence of activating FGFR3 mutations and/or FGFR3 overexpression in bladder cancer, together with a large body of preclinical evidence from loss-of-function studies, implicate FGFR3 as an important oncogenic driver and potential therapeutic target in this disease (12, 23–26). Despite recent progress toward clinical investigation of experimental agents targeting FGFR3 (27, 28), mechanistic insights into how FGFR3 signaling contributes to bladder cancer development and progression remain scarce. Here we report that FGFR3 signaling through PI3K-mTORC1 activates SREBP1 and its downstream targets to promote fatty acid synthesis and desaturation in human bladder cancer cells. Moreover, we show that in bladder cancer cells with constitutively activated FGFR3 signaling, genetic or pharmacologic intervention with fatty acid desaturation catalyzed by SCD1 substantially inhibits tumor growth in cell culture and in xenografted mice. These results uncover an important role for FGFR3-regulated fatty acid desaturation in maintaining bladder tumor growth and survival, suggesting that targeting fatty acid desaturation could be exploited in this disease setting, and possibly other cancers carrying activated FGFR3 signaling.

A striking finding from our unbiased expression analysis is that a large cohort of genes involved in sterol and fatty acid synthesis and metabolism are among the most prominently downregulated genes upon FGFR3 knockdown in bladder cancer cells. Our studies further show that ligand-induced FGFR3 activation promotes the accumulation of the cleaved active form of SREBP1 through PI3K-mTORC1 signaling, and acute pharmacologic inhibition of canonical FGFR3 signaling markedly diminishes the level of matured SREBP1 without affecting that of full length inactive SREBP1. In turn, SREBP1 induces the expression of key lipogenic enzymes and promotes *de novo* synthesis as well as desaturation of fatty acids. These results extend earlier studies showing that growth factors such as EGF, platelet-derived growth factor, and keratinocyte growth factor (KGF) are able to promote SREBP1 activation and lipogenesis in normal fibroblasts (29) and epithelial cells (37, 38), and support the notion that oncogenic growth factor receptor-SREBP1 signaling axis could be a common underpinning for the lipogenic phenotype observed in many cancer types. For example, in breast and prostate cancer cell lines activation of Her2 or EGF receptor (EGFR) induces FASN expression (39–41); in glioblastoma oncogenic EGFR signaling promotes lipogenesis by stimulating SREBP1 processing and activation (42). In addition, recent studies further suggest that

Published OnlineFirst September 26, 2012; DOI: 10.1158/0008-5472.CAN-12-1329



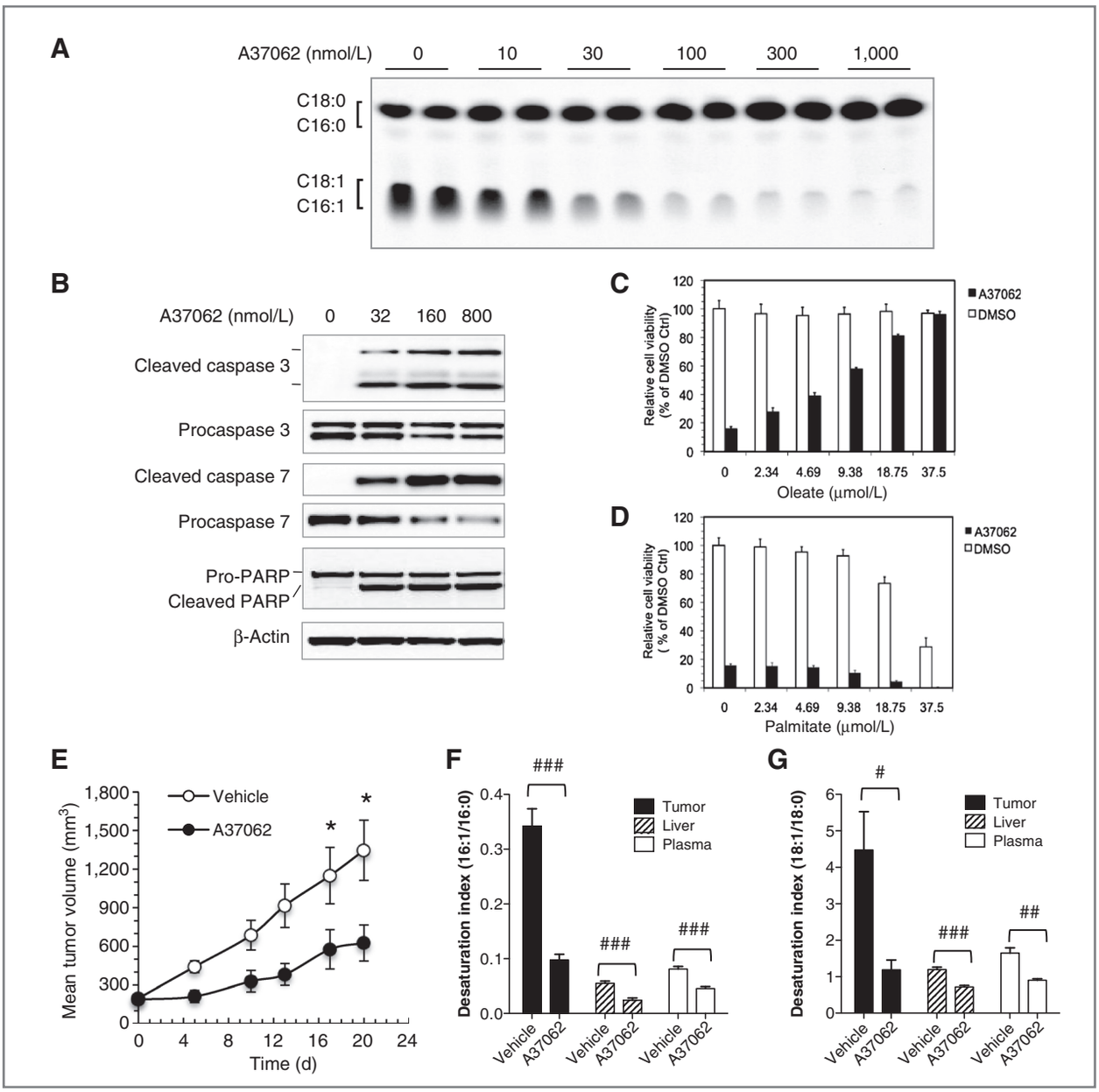


Figure 7. Pharmacologic inhibition of SCD1 attenuates tumor growth and reduces fatty acid desaturation in mice. A, SCD1 small molecule inhibitor A37062 blocks the synthesis of MUFA. UMUC-14 cells were treated with A37062 for 4 hours, then incubated with [$^{14}$C]acetate for 6 hours. Total fatty acids were extracted and separated by thin-layer chromatography. B, A37062 activates caspases 3 and 7. UMUC-14 cells were serum starved for 20 hours, then treated with A37062 for 20 hours. Cell lysates were subjected to Western blot analyses. C, monounsaturated oleate reverses growth inhibition by A37062 (100 nmol/L) in UMUC-14 cells. D, saturated palmitate fails to rescue A37062-treated UMUC-14 cells. E, SCD1 inhibitor A37062 delays xenograft growth of preestablished UMUC-14 tumors. Mice were given vehicle or A37062 (75 mg/kg) orally, twice a day, and tumor volume was presented as mean ± SEM. $n = 8$ per group. At day 17 and day 20, *, $P < 0.01$. F and G, A37062 reduces desaturation of palmitate (F) and stearate (G) in xenografted tumor tissues as well as in mouse liver and plasma at the end of the study. At 2 hours post the last treatment, samples ($n = 5$ per group) were collected and processed as described in Materials and Methods. Fatty acid methyl esters were identified by gas chromatography. Data are presented as mean ± SEM. #, $P = 0.0165$; ##, $P = 0.001$; ###, $P < 0.0006$.

activated AKT (43) or mTORC1 signaling (44) could potentiate SREBP1 processing/maturation, albeit the exact mechanisms still awaits further investigations.

Our present study for the first time also highlights the critical role of FGFR3-SREBP1 signal relay in promoting fatty acid desaturation through the induction of SCD1 expression. SCD1, the rate-limiting enzyme in fatty acid desaturation, was among the genes that showed the greatest modulation by FGFR3 knockdown in bladder cancer cells. Accordingly, FGF1 induced a pronounced increase in SCD1 expression and in

Published OnlineFirst September 26, 2012; DOI: 10.1158/0008-5472.CAN-12-1329



synthesis of unsaturated fatty acids. This regulation is mediated mainly through SREBP1, as SREBP1 siRNA markedly reduced basal and FGF1-induced SCD1 expression, whereas knockdown of SREBP2 alone had minimal effect on SCD1 expression. Importantly, our results suggest that bladder cancer cells with constitutively activated FGFR3 signaling have a greater dependence on fatty acid desaturation. In bladder cancer cells with wild type FGFR3 and/or low basal FGFR3 activation, knockdown SCD1 in general had moderate or no effect on cell proliferation. In contrast, bladder cancer cells with either a mutant FGFR3 (i.e., UMUC-14 and TCC-97-7) or constitutively active FGFR3 signaling (i.e., SW780) were more susceptible to SCD1 blockade. Inhibition of SCD1 through RNA interference or pharmacologic intervention blocked fatty acid desaturation, resulting in $G_1$ cell-cycle arrest and apoptosis and attenuating tumor growth in animal models. Moreover, exogenously supplemented oleic acid was able to rescue cells from SCD1 inhibition, confirming the importance of fatty acid desaturation for cell proliferation and survival. These results suggest that FGFR3-driven bladder tumor growth increases the demand for fatty acid desaturation, a requirement that is fulfilled by signaling through PI3K-mTORC1 to upregulate SREBP1 and SCD1 activity. Taken together, these findings identify SCD1 as a potentially attractive therapeutic target for FGFR3-driven bladder cancer.

Although therapeutic agents targeting FGFR3 directly have recently been evaluated in the clinic (27, 28), it is not yet clear whether targeting FGFR3 alone would be sufficient to achieve therapeutic benefits. In addition, as acquired resistance to targeted therapies against RTKs almost invariably develops in the clinic (45–47), identification and targeting distal FGFR3 downstream signaling effectors such as SCD1 may overcome potential resistance caused by mutations or compensatory activation of upstream signaling mediators. It remains to be determined whether a combinatorial inhibition of SCD1 and FGFR3 would further potentiate the antitumor activity.

Several recent reports suggest that SCD1 is overexpressed and essential for tumor growth in other malignancies, including lung, colon, and prostate cancer (48–50), and that the fatty acid desaturation index in prostate cancer correlates with disease progression (49). These emerging data suggest that SCD1 may play a broader role in various cancer types, perhaps in part by controlling membrane biogenesis during cell division (51), and/or affecting signal transduction of diverse pathways important for cell proliferation, survival, and stress adaptation (49, 50, 52). However, the underlying mechanisms of SCD1 upregulation in these diseases have not been delineated. Our present work suggests that oncogenic growth factor receptor may underlie SCD1 dysregulation in bladder cancer, and confers a heightened vulnerability to SCD1 inhibition in FGFR3-driven bladder cancer. Future work should focus on investigating how lipid desaturation affects cellular functions in a wide spectrum of human cancers and identifying biomarkers that could predict response to SCD1 intervention, thus providing a mechanistic basis and diagnostic approach to aid potential therapeutic targeting of SCD1.

## Disclosure of Potential Conflicts of Interest

X. Du, Q.-R. Wang, E. Chan, M. Merchant, J. Liu, D. French, A. Ashkenazi, and J. Qing are full-time employees of Genentech, Inc. No other potential conflicts of interest were disclosed.

## Authors' Contributions

**Conception and design:** A. Ashkenazi, J. Qing
**Development of methodology:** X. Du, D. French, J. Qing
**Acquisition of data (provided animals, acquired and managed patients, provided facilities, etc.):** X. Du, Q.-R. Wang, E. Chan, M. Merchant, D. French, J. Qing
**Analysis and interpretation of data (e.g., statistical analysis, biostatistics, computational analysis):** X. Du, Q.-R. Wang, E. Chan, M. Merchant, J. Liu, D. French, A. Ashkenazi, J. Qing
**Writing, review, and/or revision of the manuscript:** M. Merchant, J. Liu, D. French, A. Ashkenazi, J. Qing
**Administrative, technical, or material support (i.e., reporting or organizing data, constructing databases):** E. Chan, D. French
**Study supervision:** M. Merchant, J. Qing

## Acknowledgments

The authors thank Steven Magnuson, Jason Boggs, Po-Chang Chiang, Amy Sambrone, and Marcia Belvin for help and input on the small molecule studies, and Zora Modrusan for microarray profiling. Jonathan Zarzar helped with some initial SCD1 RNAi studies.

The costs of publication of this article were defrayed in part by the payment of page charges. This article must therefore be hereby marked *advertisement* in accordance with 18 U.S.C. Section 1734 solely to indicate this fact.

Received April 12, 2012; revised August 7, 2012; accepted September 3, 2012; published OnlineFirst September 26, 2012.

## References

1. Eswarakumar VP, Lax I, Schlessinger J. Cellular signaling by fibroblast growth factor receptors. Cytokine Growth Factor Rev 2005;16:139–49.
2. Beenken A, Mohammadi M. The FGF family: biology, pathophysiology and therapy. Nat Rev Drug Discov 2009;8:235–53.
3. Turner N, Grose R. Fibroblast growth factor signalling: from development to cancer. Nat Rev Cancer 2010;10:116–29.
4. Dailey L, Ambrosetti D, Mansukhani A, Basilico C. Mechanisms underlying differential responses to FGF signaling. Cytokine Growth Factor Rev 2005;16:233–47.
5. Ornitz DM. FGF signaling in the developing endochondral skeleton. Cytokine Growth Factor Rev 2005;16:205–13.
6. Wilkie AO. Bad bones, absent smell, selfish testes: the pleiotropic consequences of human FGF receptor mutations. Cytokine Growth Factor Rev 2005;16:187–203.
7. Chesi M, Nardini E, Brents LA, Schrock E, Ried T, Kuehl WM, et al. Frequent translocation t(4;14)(p16.3;q32.3) in multiple myeloma is associated with increased expression and activating mutations of fibroblast growth factor receptor 3. Nat Genet 1997;16:260–4.
8. Moreau P, Facon T, Leleu X, Morineau N, Huyghe P, Harousseau JL, et al. Recurrent 14q32 translocations determine the prognosis of multiple myeloma, especially in patients receiving intensive chemotherapy. Blood 2002;100:1579–83.
9. Trudel S, Ely S, Farooqi Y, Affer M, Robbiani DF, Chesi M, et al. Inhibition of fibroblast growth factor receptor 3 induces differentiation and apoptosis in t(4;14) myeloma. Blood 2004;103:3521–8.
10. Chang H, Stewart AK, Qi XY, Li ZH, Yi QL, Trudel S. Immunohistochemistry accurately predicts FGFR3 aberrant expression and t(4;14) in multiple myeloma. Blood 2005;106:353–5.
11. Cappellen D, De Oliveira C, Ricol D, de Medina S, Bourdin J, Sastre-Garau X, et al. Frequent activating mutations of FGFR3 in human bladder and cervix carcinomas. Nat Genet 1999;23:18–20.

Published OnlineFirst September 26, 2012; DOI: 10.1158/0008-5472.CAN-12-1329




12. Gomez-Roman JJ, Saenz P, Molina M, Cuevas Gonzalez J, Escuredo K, Santa Cruz S, et al. Fibroblast growth factor receptor 3 is overexpressed in urinary tract carcinomas and modulates the neoplastic cell growth. Clin Cancer Res 2005;11:459–65.
13. Tomlinson DC, Baldo O, Harnden P, Knowles MA. FGFR3 protein expression and its relationship to mutation status and prognostic variables in bladder cancer. J Pathol 2007;213:91–8.
14. van Rhijn BW, Montironi R, Zwarthoff EC, Jobsis AC, van der Kwast TH. Frequent FGFR3 mutations in urothelial papilloma. J Pathol 2002; 198:245–51.
15. Kuroso K, Imai Y, Kobayashi M, Yanagimoto K, Suzuki T, Kojima M, et al. Immunohistochemical detection of fibroblast growth factor receptor 3 in human breast cancer: correlation with clinicopathological/ molecular parameters and prognosis. Pathobiology 2010;77:231–40.
16. Rosty C, Aubriot MH, Cappellen D, Bourdin J, Cartier I, Thiery JP, et al. Clinical and biological characteristics of cervical neoplasias with FGFR3 mutation. Mol Cancer 2005;4:15–23.
17. Qiu WH, Zhou BS, Chu PG, Chen WG, Chung C, Shih J, et al. Overexpression of fibroblast growth factor receptor 3 in human hepatocellular carcinoma. World J Gastroenterol 2005;11:5266–72.
18. Woenckhaus M, Klein-Hitpass L, Grepmeier U, Merk J, Pfeifer M, Wild P, et al. Smoking and cancer-related gene expression in bronchial epithelium and non-small-cell lung cancers. J Pathol 2006;210:192–204.
19. Cortese R, Hartmann O, Berlin K, Eckhardt F. Correlative gene expression and DNA methylation profiling in lung development nominate new biomarkers in lung cancer. Int J Biochem Cell Biol 2008;40:1494–508.
20. Goriely A, Hansen RM, Taylor IB, Olesen IA, Jacobsen GK, McGowan SJ, et al. Activating mutations in FGFR3 and HRAS reveal a shared genetic origin for congenital disorders and testicular tumors. Nat Genet 2009;41:1247–52.
21. Al-Ahmadie HA, Iyer G, Janakiraman M, Lin O, Heguy A, Tickoo SK, et al. Somatic mutation of fibroblast growth factor receptor-3 (FGFR3) defines a distinct morphological subtype of high-grade urothelial carcinoma. J Pathol 2011;224:270–9.
22. Knowles MA. Novel therapeutic targets in bladder cancer: mutation and expression of FGF receptors. Future Oncol 2008;4:71–83.
23. Martinez-Torrecuadrada J, Cifuentes G, Lopez-Serra P, Saenz P, Martinez A, Casal JI. Targeting the extracellular domain of fibroblast growth factor receptor 3 with human single-chain Fv antibodies inhibits bladder carcinoma cell line proliferation. Clin Cancer Res 2005;11:6280–90.
24. Tomlinson DC, Hurst CD, Knowles MA. Knockdown by shRNA identifies S249C mutant FGFR3 as a potential therapeutic target in bladder cancer. Oncogene 2007;26:5889–99.
25. Qing J, Du X, Chen Y, Chan P, Li H, Wu P, et al. Antibody-based targeting of FGFR3 in bladder carcinoma and t(4;14)-positive multiple myeloma in mice. J Clin Invest 2009;119:1216–29.
26. Lamont FR, Tomlinson DC, Cooper PA, Shnyder SD, Chester JD, Knowles MA. Small molecule FGF receptor inhibitors block FGFR-dependent urothelial carcinoma growth *in vitro* and *in vivo*. Br J Cancer 2011;104:75–82.
27. Genentech. Trial evaluating the safety and pharmacokinetics of MFGR1877S in patients with advanced solid tumors, 2011. [cited 2012 April 10]. Available from: http://clinicaltrial.gov/ct2/show/NCT01363024.
28. Novartis. A dose escalation study in adult patients with advanced solid malignancies, 2009. [cited 2012 April 10]. Available from: http://clinicaltrials.gov/ct2/show/NCT01004224.
29. Demoulin JB, Ericsson J, Kallin A, Rorsman C, Ronnstrand L, Heldin CH. Platelet-derived growth factor stimulates membrane lipid synthesis through activation of phosphatidylinositol 3-kinase and sterol regulatory element-binding proteins. J Biol Chem 2004;279:35392–402.
30. Paton CM, Ntambi JM. Biochemical and physiological function of stearoyl-CoA desaturase. Am J Physiol Endocrinol Metab 2009;297: E28–37.
31. Horton JD, Goldstein JL, Brown MS. SREBPs: activators of the complete program of cholesterol and fatty acid synthesis in the liver. J Clin Invest 2002;109:1125–31.
32. Horton JD, Shah NA, Warrington JA, Anderson NN, Park SW, Brown MS, et al. Combined analysis of oligonucleotide microarray data from transgenic and knockout mice identifies direct SREBP target genes. Proc Natl Acad Sci U S A 2003;100:12027–32.
33. Goldstein JL, DeBose-Boyd RA, Brown MS. Protein sensors for membrane sterols. Cell 2006;124:35–46.
34. Menendez JA, Lupu R. Fatty acid synthase and the lipogenic phenotype in cancer pathogenesis. Nat Rev Cancer 2007;7:763–77.
35. Jebar AH, Hurst CD, Tomlinson DC, Johnston C, Taylor CF, Knowles MA. FGFR3 and Ras gene mutations are mutually exclusive genetic events in urothelial cell carcinoma. Oncogene 2005;24:5218–25.
36. Jemal A, Siegel R, Xu J, Ward E. Cancer statistics, 2010. CA: Cancer J Clin 2010;60:277–300.
37. Porstmann T, Griffiths B, Chung YL, Delpuech O, Griffiths JR, Downward J, et al. PKB/Akt induces transcription of enzymes involved in cholesterol and fatty acid biosynthesis via activation of SREBP. Oncogene 2005;24:6465–81.
38. Chang Y, Wang J, Lu X, Thewke DP, Mason RJ. KGF induces lipogenic genes through a PI3K and JNK/SREBP-1 pathway in H292 cells. J Lipid Res 2005;46:2624–35.
39. Swinnen JV, Heemers H, Deboel L, Foufelle F, Heyns W, Verhoeven G. Stimulation of tumor-associated fatty acid synthase expression by growth factor activation of the sterol regulatory element-binding protein pathway. Oncogene 2000;19:5173–81.
40. Yang YA, Han WF, Morin PJ, Chrest FJ, Pizer ES. Activation of fatty acid synthesis during neoplastic transformation: role of mitogen-activated protein kinase and phosphatidylinositol 3-kinase. Exp Cell Res 2002;279:80–90.
41. Kumar-Sinha C, Ignatoski KW, Lippman ME, Ethier SP, Chinnaiyan AM. Transcriptome analysis of HER2 reveals a molecular connection to fatty acid synthesis. Cancer Res 2003;63:132–9.
42. Guo D, Prins RM, Dang J, Kuga D, Iwanami A, Soto H, et al. EGFR signaling through an Akt-SREBP-1-dependent, rapamycin-resistant pathway sensitizes glioblastomas to antilipogenic therapy. Sci Signal 2009;2:ra82.
43. Porstmann T, Santos CR, Griffiths B, Cully M, Wu M, Leevers S, et al. SREBP activity is regulated by mTORC1 and contributes to Akt-dependent cell growth. Cell Metab 2008;8:224–36.
44. Duvel K, Yecies JL, Menon S, Raman P, Lipovsky AI, Souza AL, et al. Activation of a metabolic gene regulatory network downstream of mTOR complex 1. Mol Cell 2010;39:171–83.
45. Oxnard GR, Arcila ME, Chmielecki J, Ladanyi M, Miller VA, Pao W. New strategies in overcoming acquired resistance to epidermal growth factor receptor tyrosine kinase inhibitors in lung cancer. Clin Cancer Res 2011;17:5530–7.
46. Pierotti MA, Tamborini E, Negri T, Pricl S, Pilotti S. Targeted therapy in GIST: in silico modeling for prediction of resistance. Nat Rev Clin Oncol 2011;8:161–70.
47. Lovly CM, Pao W. Escaping ALK inhibition: mechanisms of and strategies to overcome resistance. Sci Transl Med 2012;4:120ps2.
48. Morgan-Lappe SE, Tucker LA, Huang X, Zhang Q, Sarthy AV, Zakula D, et al. Identification of Ras-related nuclear protein, targeting protein for xenopus kinesin-like protein 2, and stearoyl-CoA desaturase 1 as promising cancer targets from an RNAi-based screen. Cancer Res 2007;67:4390–8.
49. Fritz V, Benfodda Z, Rodier G, Henriquet C, Iborra F, Avances C, et al. Abrogation of *de novo* lipogenesis by stearoyl-CoA desaturase 1 inhibition interferes with oncogenic signaling and blocks prostate cancer progression in mice. Mol Cancer Ther 2010;9:1740–54.
50. Roongta UV, Pabalan JG, Wang X, Ryseck RP, Fargnoli J, Henley BJ, et al. Cancer cell dependence on unsaturated fatty acids implicates stearoyl-coA desaturase as a target for cancer therapy. Mol Cancer Res 2011;9:1551–61.
51. Igal RA. Stearoyl-CoA desaturase-1: a novel key player in the mechanisms of cell proliferation, programmed cell death and transformation to cancer. Carcinogenesis 2010;31:1509–15.
52. Scaglia N, Chisholm JW, Igal RA. Inhibition of stearoylCoA desaturase-1 inactivates acetyl-CoA carboxylase and impairs proliferation in cancer cells: role of AMPK. PloS One 2009;4:e6812.

Cancer Research
The Journal of Cancer Research (1916–1930) | The American Journal of Cancer (1931–1940)

AACR American Association for Cancer Research

# FGFR3 Stimulates Stearoyl CoA Desaturase 1 Activity to Promote Bladder Tumor Growth

Xiangnan Du, Qian-Rena Wang, Emily Chan, et al.

*Cancer Res* 2012;72:5843-5855. Published OnlineFirst September 26, 2012.